Lawrence Berkeley National Laboratory
Recent Work

Title
51000 T- DECAYS

Permalink
https://escholarship.org/uc/item/8zf5f5qv

Authors
Mast, Terry S.
Gershwin, Lawrence K.
Alston-Garnjost, Margaret
et al.

Publication Date
1969

eScholarship.org Powered by the California Digital Library
University of California

UCRL-18760

ey. 2
(ey 2 mcg)

RECEIVED
LAWRENCE
RADIATION LABORATORY

APR 7 1969

LIBRARY AND
DOCUMENTS SECTION

51 000 τ^- DECAYS

Terry S. Mast, Lawrence K. Gershwin,
Margaret Alston-Garnjost, Roger O. Bangerter,
Angela Barbaro-Galtieri, Joseph J. Murray,
Frank T. Solmitz, and Robert D. Tripp

January 1969

TWO-WEEK LOAN COPY

This is a Library Circulating Copy which may be borrowed for two weeks. For a personal retention copy, call Tech. Info. Division, Ext. 5545

LAWRENCE RADIATION LABORATORY
UNIVERSITY of CALIFORNIA BERKELEY

UCRL-18760

ey. 2

39a

DISCLAIMER

This document was prepared as an account of work sponsored by the United States Government. While this document is believed to contain correct information, neither the United States Government nor any agency thereof, nor the Regents of the University of California, nor any of their employees, makes any warranty, express or implied, or assumes any legal responsibility for the accuracy, completeness, or usefulness of any information, apparatus, product, or process disclosed, or represents that its use would not infringe privately owned rights. Reference herein to any specific commercial product, process, or service by its trade name, trademark, manufacturer, or otherwise, does not necessarily constitute or imply its endorsement, recommendation, or favoring by the United States Government or any agency thereof, or the Regents of the University of California. The views and opinions of authors expressed herein do not necessarily state or reflect those of the United States Government or any agency thereof or the Regents of the University of California.

To be submitted to Physical Review

UCRL-18760
Preprint

UNIVERSITY OF CALIFORNIA

Lawrence Radiation Laboratory
Berkeley, California

AEC Contract No. W-7405-eng-48

51 000 τ^- DECAYS

Terry S. Mast, Lawrence K. Gershwin, Margaret Alston-Garnjost, Roger O. Bangerter, Angela Barbaro-Galtieri, Joseph J. Murray, Frank T. Solmitz, and Robert D. Tripp

January 1969

51 000 τ^- DECAYS*

Terry S. Mast, Lawrence K. Gershwin, Margaret Alston-Garnjost, Roger O. Bangerter, Angela Barbaro-Galtieri, Joseph J. Murray, † Frank T. Solmitz, and Robert D. Tripp

Lawrence Radiation Laboratory
University of California
Berkeley, California

January 1969

Abstract

An analysis has been made of 51 000 $K^- \rightarrow \pi^-\pi^-\pi^+$ decays in flight in the Berkeley 25-inch hydrogen bubble chamber. After corrections for detection efficiency and Coulomb interactions, the projections of the pion spectra have been fitted to expansions in the Dalitz variables x and y. In addition, maximum-likelihood fits to the entire Dalitz plot have been made. The decay distribution is well described by $1 + ay$, where the slope $a = 0.247 \pm 0.009$. Comparison of this slope with that derived from a world compilation of 28 000 τ^+ decays shows no evidence for CP violation. An isospin analysis of the rates and slopes of τ, τ', and $K_2^0 \rightarrow 3\pi$ decays requires, in addition to the dominant $\Delta I = 1/2$ amplitude, $\Delta I = 3/2$ amplitudes into both $I = 1$ and $I = 2$ three-pion final states. No detectable $\Delta I = 5/2$ or $\Delta I = 7/2$ amplitudes are required.

I. Introduction

Since the first analysis of τ meson data consisting of 13 events,[1] it has been known that the energy distribution of the three pions is governed largely by phase space. By 1957 analysis of a compilation of 892 τ^+ decays[2] showed that a fit linear in the kinetic energy of the odd pion adequately described the small deviation from uniformity of the Dalitz plot. Since then a number of experiments, each generally consisting of several thousand events, have confirmed this simple structure. In this experiment we report a measurement of the pion spectra for a sample of τ^- which is nearly an order of magnitude larger than any heretofore reported. The results are in agreement with previous measurements, and no structure beyond a term linear in the odd-pion energy is observed.

Section II of this paper describes the experimental procedures followed and the bias corrections applied to the data. Section III contains a tabulation of the Dalitz plot and graphs of its projections weighted to remove the effect of final-state Coulomb interactions. Results of a variety of ways of fitting the data are contained in Tables I and II.

If the weak interaction responsible for τ decay is CP invariant, the spectra of τ^+ and τ^- decay should be identical. In Section IV a comparison is made of a world summary of the data for each charge, and no detectable difference in these spectra is found.

In order to explore the isospin dependence of the decay amplitude one must compare the rates or slopes (or both) of τ decay ($K^\pm \to \pi^\pm\pi^+\pi^-$) with other three-pion decay modes of the K meson,

such as τ' decay ($K^+ \to \pi^+\pi^0\pi^0$) and the neutral K decays $K_2^0 \to \pi^+\pi^-\pi^0$ and $K_2^0 \to 3\pi^0$. Since 1956, when Dalitz made the first comparison of τ and τ' decay rates,[3] it has been apparent that the 3π decay of the K meson can be described by a dominant $\Delta I = 1/2$ amplitude although varying experimental data have usually required small admixtures of other amplitudes. In 1960 Weinberg[4] suggested a comparison of the τ and τ' slopes as another test of the $\Delta I = 1/2$ rule. In Section IV we use the most recent data compilation on the decay rates[5] in conjunction with our compilation of slopes (Table III) to show that $\Delta I = 3/2$ amplitudes into both $I = 1$ and $I = 2$ three-pion final states are required when conventional prescriptions for multiplet mass differences are employed, and exhibit graphically the limits placed on these amplitudes by the data.

II. Experimental Analysis

An exposure of 1.3×10^6 pictures in the Berkeley 25-inch hydrogen bubble chamber has yielded about 60 000 $K^- \to \pi^-\pi^-\pi^+$ decays in flight. The K^- momenta range from 270 to 470 MeV/c.

After a complete first scan a third of the film was rescanned, and this indicated an overall scanning efficiency of about 96%. Scanners were instructed to isolate those events that on the basis of ionization had a definite e^+ or e^- as a visible decay product. A fraction of the 3380 events isolated were more closely inspected, and a negligible number were found to be three-pion decays. All the isolated events were removed from the sample and the remaining events were measured. A restricted fiducial volume for the decay vertex was defined to insure sufficient length of tracks for a good measurement. This restriction

reduced our sample to 52 715 events. Events for which the measurement did not satisfy energy and momentum conservation adequately were remeasured until a total of 52 261 events passed with a confidence level greater than 0.001. Half of these events had been measured on Franckensteins and half on a Spiral Reader. About 0.5% of the events passed both the four-constraint fit to $K \rightarrow \pi^-\pi^-\pi^+$ and the two-constraint fit to $K^- \rightarrow \pi^-\pi^0$, $\pi^0 \rightarrow e^+e^-\gamma$. Reexamination of these events showed them all to be three-pion decays, and they were retained in the sample. About 400 events fitted only the hypothesis $K^- \rightarrow \pi^- \pi^0$, $\pi^0 \rightarrow e^+e^-\gamma$. Combining these with the events originally isolated by the scanners gives a total of 3780, in approximate agreement with the number expected from known branching ratios.

In order to estimate the amount of $3\pi\gamma$ contamination, about 4000 events were fitted to both $K^- \rightarrow 3\pi$ and $K^- \rightarrow 3\pi\gamma$. The number fitting $3\pi\gamma$ with a γ energy greater than 10 MeV was in rough agreement with predictions by Dalitz.[6] Another experiment, by Stamer et al.,[7] indicates a branching fraction that is also in agreement with Dalitz' s calculations. On the basis of these predictions we expect in our total sample about 50 events with a photon energy greater than 10 MeV. Our fit of the 4000 events indicates that most of the $3\pi\gamma$ events would not pass the criteria for 3π events.

A comparison of the measured pion laboratory-frame momentum distribution with a Monte Carlo calculation showed that the scanners missed about 45% of the events with a pion momentum less than 30 MeV/c (0.5 cm range) and about 6% of the events with a pion momentum between 30 and 60 MeV/c. A cut was made to eliminate from the sample

events in which the momentum of any pion was less than 30 MeV/c. To account for this cut each of the remaining events was weighted by a factor $1/(1-p)$, where p is the probability that any one pion has a lab momentum less than 30 MeV/c. This probability is the fraction of the pion's angular distribution in the K^- rest frame removed by the cut; it is a function of the incident momentum and the event's position in the Dalitz plot. The probability that two pions both had a momentum less than 30 MeV/c was negligible. The cut removed 944 events, and the total number of remaining weighted events was 52 625. The distribution of "short pion" weights as a function of Dalitz plot position for our events is shown in Fig. 1. An analysis of the Dalitz plot of those events with a pion of lab momentum between 30 and 60 MeV/c showed that the small fraction of these missed would have a negligible effect on the analysis of the Dalitz plot of the entire sample.

Three-pion decay is completely described by five independent variables: two energies, which determine the Dalitz plot coordinates, and three angles, which determine the orientation of the decay plane. The angles are defined in the K^- rest frame (Fig. 2) as $\cos\theta$, the polar cosine of the normal to the decay plane with respect to the beam; ϕ, the azimuth of the normal about the beam direction; and α, the azimuth of the π^+ about the normal. In the rest frame of the K^- the distributions in ϕ, α, and $\cos\theta$ should be flat. Due to the transformation from the laboratory to the K^- rest frame the cut on short pions destroys the isotropy of the distributions in α and $\cos\theta$. The anisotropy we observe in these distributions can be fully explained as a result of the short-pion cut (Figs. 3a and b). The distribution in ϕ, however, is unaffected

by the weight for short pions. Investigation of this distribution showed that scanners missed some events where the edge of the decay plane faced the cameras. (Figure 3c). The distribution was folded to remove the left-right and up-down symmetries and was fitted between 0 and $\pi/2$ to a polynomial in ϕ, $1-b\phi^2$. The parameter b was found to be independent of the Dalitz plot position and equal to 0.02. Since the effect is independent of Dalitz plot position, it does not affect the analysis of the spectra. In summation, the actual number of events used to obtain the spectra is 50 919, which when weighted for the loss of low-momentum pions gives 52 625 weighted events which have an average weight of 1.034.

III. Fits to the Pion Spectra

To compare spectra of various charged modes of K decay and to compare data with theoretical predictions, many experimenters have weighted their distributions to account for the effects of final-state Coulomb interactions. There is some question about the appropriate prescription to be used, and different authors have used different expressions. Consequently we have fitted our data both with and without these corrections. Following Dalitz[3] and Schiff[8] it is assumed that the Coulomb interaction between pions i and j multiplies the phase space by a factor $n/(e^n-1)$, where $n = 2\pi e_i e_j/v_{ij}$ and v_{ij} is the relativistic relative velocity between pions i and j. The distribution of Coulomb weights over the Dalitz plot is shown in Fig. 4.

The usual variables x and y are defined from the pion kinetic energies in the K^- rest frame,

$$x = \frac{\sqrt{3}}{Q} |T_1 - T_2| \text{ and } y = \frac{1}{Q}(3T_3 - Q),$$

where T_1, T_2, and T_3 are the kinetic energies of the negative pions and positive pion respectively, and $Q = M_K - 3m_\pi$.

Figure 5a shows the array of the events over the Dalitz plot with statistical errors. The events have been weighted for the short-pion cut. The events of Fig. 5b have in addition been weighted for Coulomb interactions.

The normal kinematic fitting of the measured events gives uncertainties in laboratory-system quantities. In order to calculate the uncertainties in the center-of-mass quantities x and y, a sample of about 2000 events was fitted to the hypotheses $K^- \rightarrow$ pion + missing mass, missing mass $\rightarrow$ two pions. These fits give the uncertainties in the three combinations of dipion invariant masses, and these can be related to the K^- rest frame quantities x and y. The mean errors in the x and y positions varied from 0.01 to 0.025 over the Dalitz plot.

For comparison with previous results the x and y projections of the Dalitz plot have been fitted, by using a least-squares method, to expansions in x^2 and y. Uncertainties in the x and y positions cause large uncertainties in the weighting for phase space at large x and y in these projections. To remove this uncertainty the last bins of the x and y projections were cut at 0.961 and 0.920 respectively, and the events in these bins were weighted to account for the cut. Table I summarizes the least-squares fits to these projections, both with and without weights for Coulomb interactions. The distribution in y (Fig. 6) is well described by the linear fit. The distribution in x (Fig. 7) has been weighted by $1/(1 + 0.247\,y)$ to remove the reflected y dependence. The low confidence levels for the x fits are due to a presumed

statistical fluctuation at $x = 0.6$. Although there is a two-standard-deviation x^2 dependence, the quality of the fit is not substantially improved by the introduction of this x^2 dependence.

A y^2 term in the spectrum can be generated by the square of a linear term in the matrix element and by the interference between constant and quadratic terms in the matrix element. A linear matrix element which reproduces the y dependence of our spectrum would generate a quadratic term approximately equal to $+ 0.015\ y^2$. Our observed y^2 dependence, $(-0.023 \pm 0.019)y^2$, differs by two standard deviations from this, suggesting the possible presence of a negative quadratic term in the matrix element.

In a search for other structure we have made a maximum-likelihood fit to the entire Dalitz plot. The results of a five-parameter fit are shown in Table IIA. Again the only significant structure is the linear term in y. To test the quality of the fit the data were divided into bins and the final fit integrated over each bin. A χ^2 of 341 was then calculated for the 313 degrees of freedom. A similar fit has been made in the variables ρ and θ suggested by Weinberg.[4] Here $x = \rho \sin\theta$ and $y = \rho \cos\theta$. An expansion up to $\rho \cos\theta$ corresponds to a linear y expansion; however, higher-order terms differ from the expansion in x and y. The results are shown in Table IIB, and again the only significant structure corresponds to a linear term in $\rho \cos\theta$ or in y.

We have investigated the y dependence of those events with a confidence level less than 0.01, and found it consistent with the rest of the sample. We have also found agreement between the y distributions

for those events measured on the Spiral Reader and those measured on the Franckenstein. As a final check we have made a number of least-squares fits to the form 1 + ay looking for dependence of a on the incident momentum, the three decay angles, or the position of the event in the chamber. These fits show (as expected) no dependence on those variables. (Fig. 8).

Our results are combined with previous results in Table III.[9] For the comparison of various charged modes, mass differences within the K and π multiplets introduce important corrections. For this reason a more appropriate parameter g, the coefficient of an invariant, has been defined by

$$M^2 = 1 + g \frac{s_3 - s_0}{m_{\pi^+}^2} .$$

Here $s_i = (p_K - p_i)^2$ and $s_0 = (s_1+s_2+s_3)/3$, and we have introduced the charged pion mass so as to make g dimensionless. For τ decay, in which the pion masses are equal, the invariant term is related to y by

$$s_3 - s_0 = - 2 M_K Q y/3 .$$

IV. $K \rightarrow 3\pi$ Amplitudes

A difference in the Dalitz plots of $K^- \rightarrow \pi^-\pi^-\pi^+$ and $K^+ \rightarrow \pi^+\pi^+\pi^-$ would be an indication of CP violation in this decay. Following Wolfenstein,[10] we parameterize the difference in the slopes for τ^- and τ^+ as

$$\Delta = \frac{a(\tau^+) - a(\tau^-)}{a(\tau^+) + a(\tau^-)}$$

and calculate, from Table III, $\Delta = 0.024 \pm 0.031$. A number of models for CP violation have been proposed, and most of them predict[10] $\Delta \lesssim 10^{-3}$.

We now turn to a comparison of the presently available data on decay rates and the odd-pion spectra for the four decays $K^{\pm} \to \pi^{\pm}\pi^{+}\pi^{-}$, $K^{+} \to \pi^{+}\pi^{0}\pi^{0}$, $K_2^0 \to \pi^{0}\pi^{+}\pi^{-}$, $K_2^0 \to 3\pi^{0}$. In this discussion we follow Zemach,[11] who has made a general analysis of the isospin decomposition for these decays. The amplitudes used in this analysis are summarized in Table IV. The subscripts "ch" and "n" on these amplitudes refer to charged and neutral K decays, which can in turn be expressed as linear combinations of the two ΔI transitions of which each is composed. Columns 4 and 5 of Table IV list these expressions. The numerical subscript is 2 ΔI. Table V gives a summary of the data on the three ratios of reduced decay rates (γ) and the three slopes (g). The ratios of the reduced rates were calculated by using Coulomb-corrected nonuniform Dalitz plot phase-space factors to correct for mass and charge differences[12] and rates taken from the compilation of the Particle Data Group.[5] The ratios have been factored to show the deviations from the predictions of the $\Delta I = 1/2$ rule, for which the value in the parenthesis should be 1.00. The slopes of the spectra are from Table III. In addition to the experimental data, Table V also contains expressions for the decay rates and slopes in terms of various coefficients of the decay amplitudes, which can be found in Ref. 11.

Equations (1) and (2) of Table V imply that the ratios of the amplitudes leading to I = 3 final states to the amplitudes leading to I = 1 final states lie on circles in the complex plane (Fig. 9a, b). These ratios are consistent with the vanishing of the I = 3 amplitudes, and in the following calculations we have assumed them to be zero. The third

equation implies that the ratio of the I = 1, $\Delta I = 3/2$ amplitude to the I = 1, $\Delta I = 1/2$ amplitudes also lies on a circle in the complex plane (Fig. 9c). If CP invariance is assumed and final-state interactions are neglected[13] these amplitudes are real, and this ratio has either of two values, 0.032 ± 0.006 or 1.75 ± 0.05. Although there is no direct evidence favoring the smaller value in $K \to 3\pi$, the success of the dominant $\Delta I = 1/2$ rule in $K \to 2\pi$ and other nonleptonic strange-particle decays obviously suggests the former.

The data on the slopes (Eqs. 4 and 5 of Table V) imply that $\mathrm{Re}(c_{ch}/a_{ch})$ equals 0.029 ± 0.005. If the ratios of the I = 1 parameters are defined as

$$U = (a_3/a_1), \quad V = (b_1/a_1), \quad W = (b_3/a_1),$$

relations (4), (5), and (6) yield for V and W, for the value of $U = 0.032 \pm 0.006$ determined from the rates, the values

$$V = 0.218 \pm 0.006, \quad W = 0.015 \pm 0.006.$$

In conclusion, the current data on $K \to 3\pi$ exhibit the following isospin properties:

(a) A comparison of τ and τ' rates and a comparison of $K_2^0 \to \pi^+\pi^-\pi^0$ with $K_2^0 \to 3\pi^0$ show that I = 3 final states are not required.

(b) A $\Delta I = 3/2$, I = 1 amplitude ($a_3/a_1 = 0.032 \pm 0.006$) is indicated by the $K_2^0 \to \pi^+\pi^-\pi^0$ decay rate's being too low by four standard deviations with respect to the rate for $K^\pm \to \pi^\pm\pi^+\pi^-$ to be consistent with the $\Delta I = 1/2$ rule.

(c) An I = 2 ($\Delta I = 3/2$ or $5/2$) amplitude ($c_{ch}/a_{ch} = +0.029 \pm 0.005$) arises from the τ' slope's being 6.5 standard deviations larger than is expected from the τ slope and the $\Delta I = 1/2$ rule.

(d) The slopes of the three Dalitz plots show the presence of an $I = 1$ state of mixed symmetry. From comparison of the τ and τ' slopes with the K_2^0 slope this state is found to come predominantly from $\Delta I = 1/2$ ($b_1/a_1 = +0.218 \pm 0.006$) with a small admixture of $\Delta I = 3/2$ ($b_3/a_1 = +0.015 \pm 0.006$).

It is important to reemphasize that the above quantitative results are based on the neglect of final-state interactions, which do give rise to imaginary parts to the amplitudes. In addition, the prescriptions we have used to account for Coulomb effects and mass differences are subject to theoretical uncertainty.

Acknowledgments

We express our appreciation to Mr. Glenn Eckman and the crew of the 25-inch bubble chamber and to Mr. Roger Gearhart. We are especially grateful to those responsible for the development and the operation of the Spiral Reader, in particular Dr. Gerald Lynch. We also gratefully acknowledge helpful discussions with Professor J. D. Jackson. In addition, we acknowledge the continuing interest of Professor Luis W. Alvarez.

Footnotes and References

*Work done under the auspices of the U. S. Atomic Energy Commission.

†Present address: SLAC, Stanford, California.

1. R. H. Dalitz, Phil. Mag. 44, 1068 (1953).

2. R. H. Dalitz, Rept. Progr. Phys. 20, 163 (1957).

3. R. H. Dalitz, Proc. Phys. Soc. (London) 69A, 527 (1956).

4. S. Weinberg, Phys. Rev. Letters 4, 87 (1960).

5. Particle Data Group, Lawrence Radiation Laboratory Report UCRL-8030 Rev., Jan. 1969.

6. R. H. Dalitz, Phys. Rev. 99, 5,915 (1955).

7. P. Stamer, T. Huetter, E. L. Koller, S. Taylor, and J. Grauman, Phys. Rev. 138B, 400 (1965).

8. L. I. Schiff, Quantum Mechanics (McGraw-Hill Book Co., Inc., New York, p. 116.

9. This compilation includes only experiments with greater than 1000 events. The experiment of Ferro-Luzzi et al. has not been included in the τ^- average, since the analysis did not include factors accounting for final-state Coulomb interactions. The result of Hopkins et al. has not been included in the K_2^0 average, since the value differs by more than five standard deviations from the weighted average of the other two results. In addition, their spectrum is quite sensitive to their estimation of a large K_{e3} and $K_{\mu 3}$ background. The experiments on K_2^0 have all used a nonrelativistic expression for the matrix element and we have renormalized their results to obtain the coefficient g. Furthermore, these analyses have not applied corrections for final-state

Coulomb interactions; however, we estimate the effect on the results to be negligible.

10. L. Wolfenstein, "Ettore Majorana" Summer School Notes, 1968.

11. C. Zemach, Phys. Rev. 133B, B1201-1220 (1964).

12. The experimental rates of the January 1969 compilation of the Particle Data Group have been used (Ref. 5). We have recalculated the phase-space factors, using a completely relativistic formulation, and using as inputs the masses from the above compilation and the slopes of the Dalitz plots from Table V of this paper. The values are

	Method		
	UDP	NUDP	CNUDP
$\phi_1(000)$	1.487	1.487	1.451
$\phi_2(+-0)$	1.219	1.268	1.268
$\phi_3(++-)$	1.000	1.000	1.000
$\phi_4(+00)$	1.247	1.184	1.155

The factors labeled UDP are the relative areas of the Dalitz plots assuming a uniform distribution. The factors labeled NUDP include the observed slopes from Table V. The factors for the decays with equal-mass pions are unaffected by the inclusion of a slope. Those labeled CNUDP result from also including final-state Coulomb interactions according to the prescription described in the text. These factors (UDP and NUDP) have also been calculated by T. Devlin, Phys. Rev. Letters 20, 683 (1968) and B. G. Kenny, Phys. Rev. 175, 2054 (1968).

13. Schult and Barbour have calculated the τ and τ' slopes from the effects of final-state strong interactions, using a model based on the Faddeev equations. The phase of their matrix element at the center of the Dalitz plot is about 14 deg. See Barbour and Schult, Phys. Rev. 155, 1712 (1967) and Phys. Rev. 164, 1791 (1967).

14. M. L. Moscoso, thesis, University of Paris, Centre d'Orsay.

15. M. Ferro-Luzzi, D. H. Miller, J. J. Murray, A. H. Rosenfeld, and R. D. Tripp, Nuovo Cimento 22, 1087 (1961).

16. W. R. Butler, R. W. Bland, G. Goldhaber, S. Goldhaber, A. A. Hirata, T. O'Halloran, G. H. Trilling, and C. G. Wohl, UCRL-18420 and Addendum, August, 1968.

17. J. Grauman, E. L. Koller, S. Taylor, D. Pandoulas, and S. Hoffmaster, Bull. Am. Phys. Soc. 13, 586 (1968), and Stevens Institute of Technology Report P216.

18. R. J. Plano (Rutgers University), invited talk, APS meeting, New York, Jan. 1967, and private communication.

19. T. Huetter, S. Taylor, E. L. Koller, P. Stamer, and J. Grauman, Phys. Rev. 140, B655 (1965).

20. D. Davison, R. Bacastow, W. H. Barkas, D. A. Evans, S.-Y. Fung, L. E. Porter, R. T. Poe, and D. Greiner, University of California—Riverside Report UCR-34P 107-74, October 7, 1968.

21. V. Bisi, G. Borreani, R. Cester, A. DeMarco-Trabuco, M. Ferrero, C. Garelli, A. Chiesa, B. Quassiati, R. Rinando, M. Vigone, and A. Werbrouck, Nuovo Cimento 35, 768 (1965).

22. G. E. Kalmus, A. Kernan, R. T. Pu, W. M. Powell, and R. Dowd, Phys. Rev. Letters 13, 99 (1964).

23. P. Basile, J. W. Cronin, B. Thevenet, R. Turlay, S. Zylberajch, and A. Zylbersztejn, Phys. Letters 28B, 58 (1968).

24. H. W. K. Hopkins, T. C. Bacon, and F. R. Eisler, Phys. Rev. Letters 19, 185 (1967).

25. B. M. K. Nefkens, A. Abashian, R. J. Abrams, D. W. Carpenter, G. P. Fisher, and J. H. Smith, Phys. Rev. 157, 1233 (1967).

Table I. Fits to X and Y projections.

A. Fit of the Y projection to $1 + ay + by^2$			Confidence level
Coulomb factor included	a	b	
Linear fit	0.247 ± 0.009	-	82.8%
Quadratic fit	0.245 ± 0.009	-0.023 ± 0.019	77.8%
No Coulomb factor			
Linear fit	0.211 ± 0.009	-	6.4%
Quadratic fit	0.205 ± 0.009	-0.042 ± 0.019	15.2%

B. Fit of the X projection to $1 + cx^2 + dx^4$			
Coulomb factor included	c	d	
Constant	-	-	0.06%
Quadratic	-0.037 ± 0.019	-	0.13%
Quartic	-0.032 ± 0.060	0.006 ± 0.080	0.08%
No Coulomb factor			
Constant	-	-	0.14%
Quadratic	-0.002 ± 0.019	-	0.09%
Quartic	-0.010 ± 0.061	-0.011 ± 0.082	0.05%

Table II. Maximum-likelihood fits to Dalitz plot.

A. Fit to $1 + ay + by^2 + cx^2 + dx^4 + ex^2y$

$a = 0.244 \pm 0.013$

$b = -0.002 \pm 0.020$

$c = -0.067 \pm 0.060$

$d = 0.069 \pm 0.083$

$e = 0.023 \pm 0.054$

error matrix ($\times$ 100)

0.0159	0.0080	0.0024	0.0021	-0.0451
	0.0401	0.0120	0.0020	-0.0152
		0.3630	-0.4705	0.0362
			0.6880	-0.0708
				0.2940

B. Fit to $1 + a\rho\cos\theta + b\rho^2\cos^2\theta + c\rho^2 + d\rho^3\cos\theta + e\rho^3\cos^3\theta$

$a = 0.219 \pm 0.027$

$b = 0.021 \pm 0.024$

$c = -0.021 \pm 0.020$

$d = 0.059 \pm 0.059$

$e = -0.015 \pm 0.057$

error matrix ($\times$ 100)

0.0072	-0.0060	0.0030	-0.01059	0.0030
	0.0565	-0.276	0.0082	0.0108
		0.0213	-0.0115	0.0130
			0.3547	-0.2433
				0.3206

Table III. Compilation of experimental results.

	Events	Reference	a	g
τ^-	50 919	This experiment	0.247 ± 0.009	
	5 778	Moscoso, 14	0.242 ± 0.029	
	1 347	Ferro-Luzzi, 15	0.28 ± 0.045	
	58 044	average =	0.247 ± 0.009	-0.194 ± 0.007
τ^+	9 994	Butler et al., 16	0.277 ± 0.020	
	6 752	Grauman et al., 17	0.228 ± 0.030	
	5 428	Plano, 18	0.28 ± 0.03	
	3 587	Huetter et al., 19	0.21 ± 0.04	
	25 761	average =	0.259 ± 0.013	-0.204 ± 0.011
τ'	4 048	Davison et al., 20		0.516 ± 0.020
	1 874	Bisi et al., 21		0.586 ± 0.098
	1 792	Kalmus et al., 22		0.48 ± 0.04
	7 714	average =		0.511 ± 0.018
K^0_2	2 446	Basile et al., 23		0.382 ± 0.040
	1 350	Hopkins et al., 24		0.651 ± 0.044
	1 198	Nefkens et al., 25		0.437 ± 0.057
	4 994	average from Refs. 23 and 25 =		0.400 ± 0.033

Table IV. $K \to 3\pi$ amplitudes classified by final-state isospin (I) and by ΔI rules.

Amplitudes	I	ΔI	$K^{\pm}$	K_2^0
a + bs	1	1/2, 3/2	$a_{ch} = a_1 + a_3$	$a_n = a_1 - 2a_3$
			$b_{ch} = b_1 + b_3$	$b_n = b_1 - 2b_3$
cs	2	3/2, 5/2	$c_{ch} = c_3 + c_5$	
d	3	5/2, 7/2	$d_{ch} = d_5 + d_7$	$d_n = 3/2 d_5 - 2d_7$

s is related to the customary invariants by

$$s = \frac{s_3 - s_0}{m_{\pi^+}^2}, \text{ where } s_i = (p_K - p_i)^2 \text{ and } s_0 = (s_1 + s_2 + s_3)/3$$

Table V. $K \to 3\pi$ rates and slopes.

	Eq. No.
$\frac{\gamma(\pm\,+\,-)}{\gamma(0\;0\;+)} = \left\lvert \frac{2a_{ch} + d_{ch}}{a_{ch} - 2d_{ch}} \right\rvert^2 = 4(0.95 \pm 0.03)$	(1)
$\frac{\gamma(0\;0\;0)}{\gamma(+\;-\;0)} = \frac{1}{6} \left\lvert \frac{3a_n - 2d_n}{a_n + d_n} \right\rvert^2 = \frac{3}{2}(0.99 \pm 0.04)$	(2)
$\frac{\gamma(\pm\,+\,-)}{\gamma(+\;-\;0)} = \frac{1}{2} \left\lvert \frac{2a_{ch} + d_{ch}}{a_n + d_n} \right\rvert^2 = 2(1.21 \pm 0.05)$	(3)
$g(0\;0\;+) = 2\mathrm{Re}\left[\frac{b_{ch} + c_{ch}}{a_{ch}}\right] = 0.511 \pm 0.018$	(4)
$g(\pm\,+\,-) = -\mathrm{Re}\left[\frac{b_{ch} - c_{ch}}{a_{ch}}\right] = -0.197 \pm 0.006$	(5)
$g(+\;-\;0) = \mathrm{Re}\left[\frac{2b_n}{a_n}\right] = 0.400 \pm 0.033$	(6)

Figure Captions

Fig. 1. Contour map showing the variation over the Dalitz plot of the weight for the loss of low-momentum pions.

Fig. 2. Figure defining the K^- rest frame angles ϕ, α, and θ.

Fig. 3. (a) and (b). Distributions in α and cos θ. The upper data have been corrected for the loss of low-momentum pions.

(c) Distribution in ϕ. The lower data are before the application of weights for azimuthal loss, the upper data after.

Fig. 4. Contour map showing the variation of the factor multiplying phase space to account for final-state Coulomb interactions.

Fig. 5. Array of the Dalitz-plot distribution of events and statistical errors. In a the events have been weighted for the loss of low-momentum pions. In b the events have in addition been weighted for the effects of final-state Coulomb interactions. The axes are divided into equal intervals.

Fig. 6. Distribution in y weighted for phase space, Coulomb interactions, and a cut on low-momentum pions. The line is a best fit to $1 + ay$, where $a = 0.247 \pm 0.009$.

Fig. 7. Distribution in x weighted for phase space, Coulomb interactions, a cut on low-momentum pions, and by $1/(1+0.247y)$.

Fig. 8. Dalitz-plot slope a from fits to the form $1 + ay$ as determined from different data samples for various intervals of incident momentum, ϕ, α, cos θ, and the distance (cm) along the beam from the center of the chamber.

Fig. 9. Plots of the allowed complex values of the ratios of various amplitudes as determined from the ratios of rates 1, 2, and 3,

respectively of Table V. (a) d_{ch}/a_{ch}, (b) d_n/a_n, (c) a_3/a_1. For plot (c) d_{ch} and d_n are assumed to vanish.

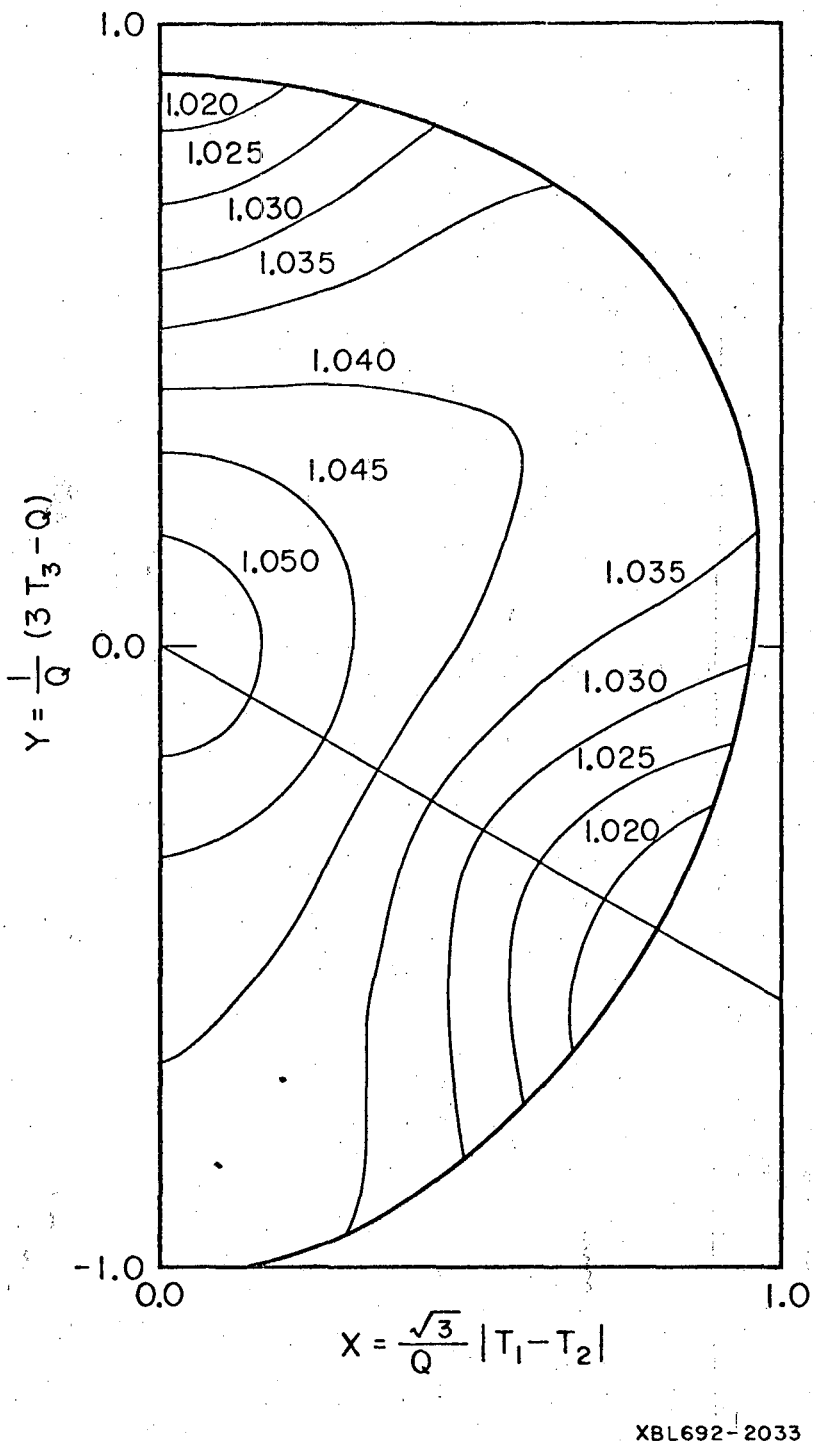
1.0
1.020
1.025
1.030
1.035
1.040
1.045
1.050
1.035
1.030
1.025
1.020
0.0
-1.0
0.0
1.0
$Y = \frac{1}{Q}(3T_3 - Q)$
$X = \frac{\sqrt{3}}{Q}|T_1 - T_2|$
XBL692-2033

Fig. 1

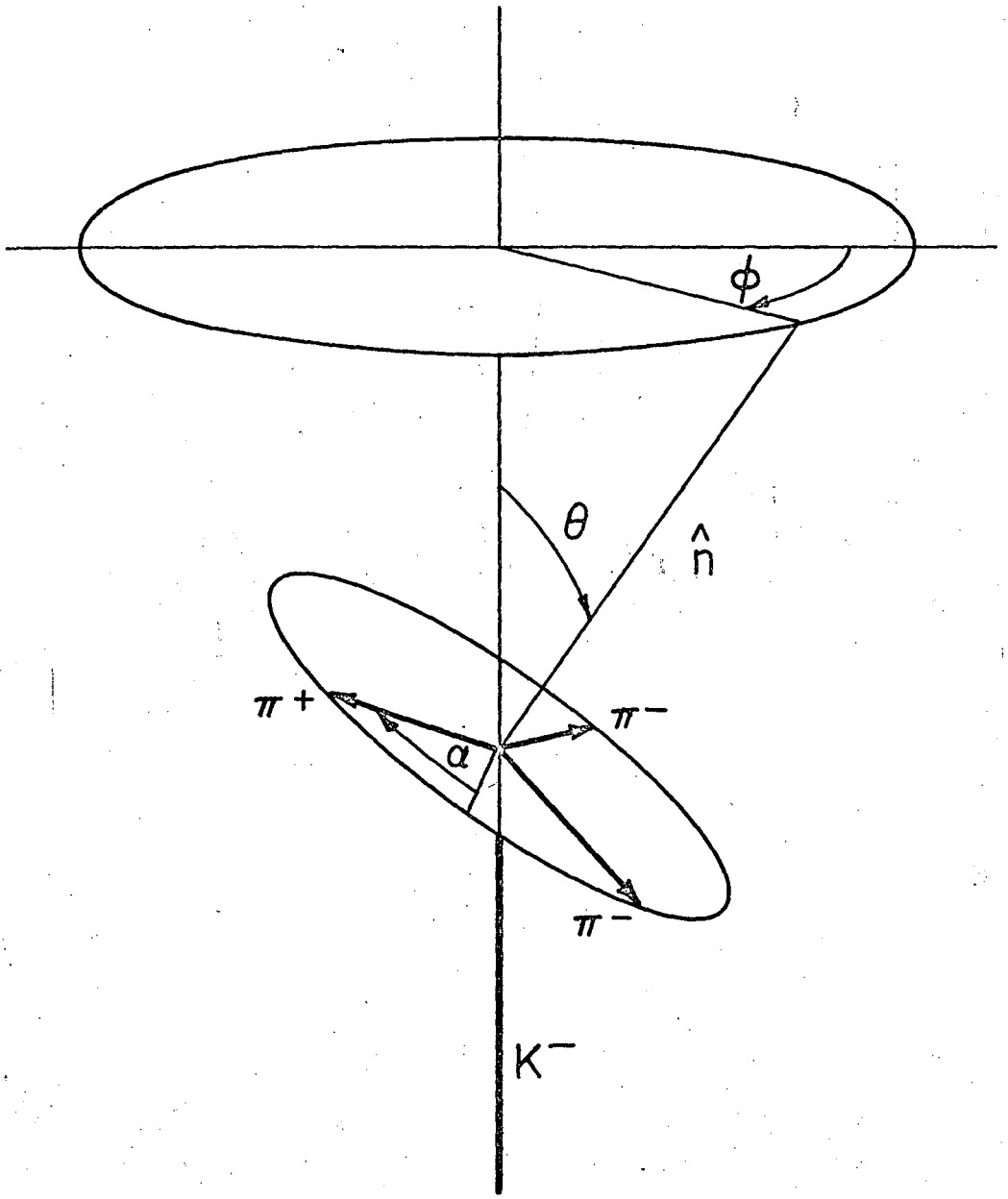

Fig. 2

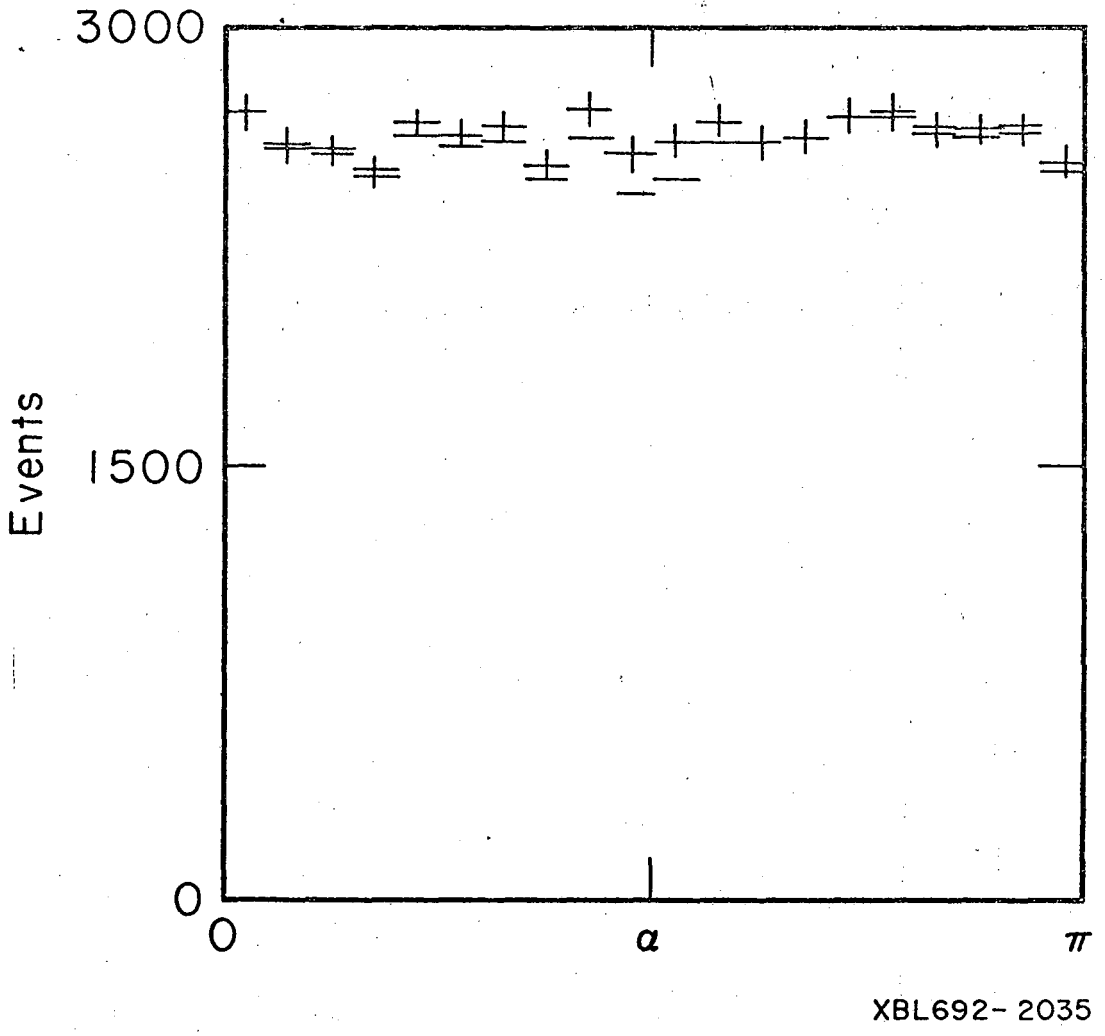

Fig. 3a

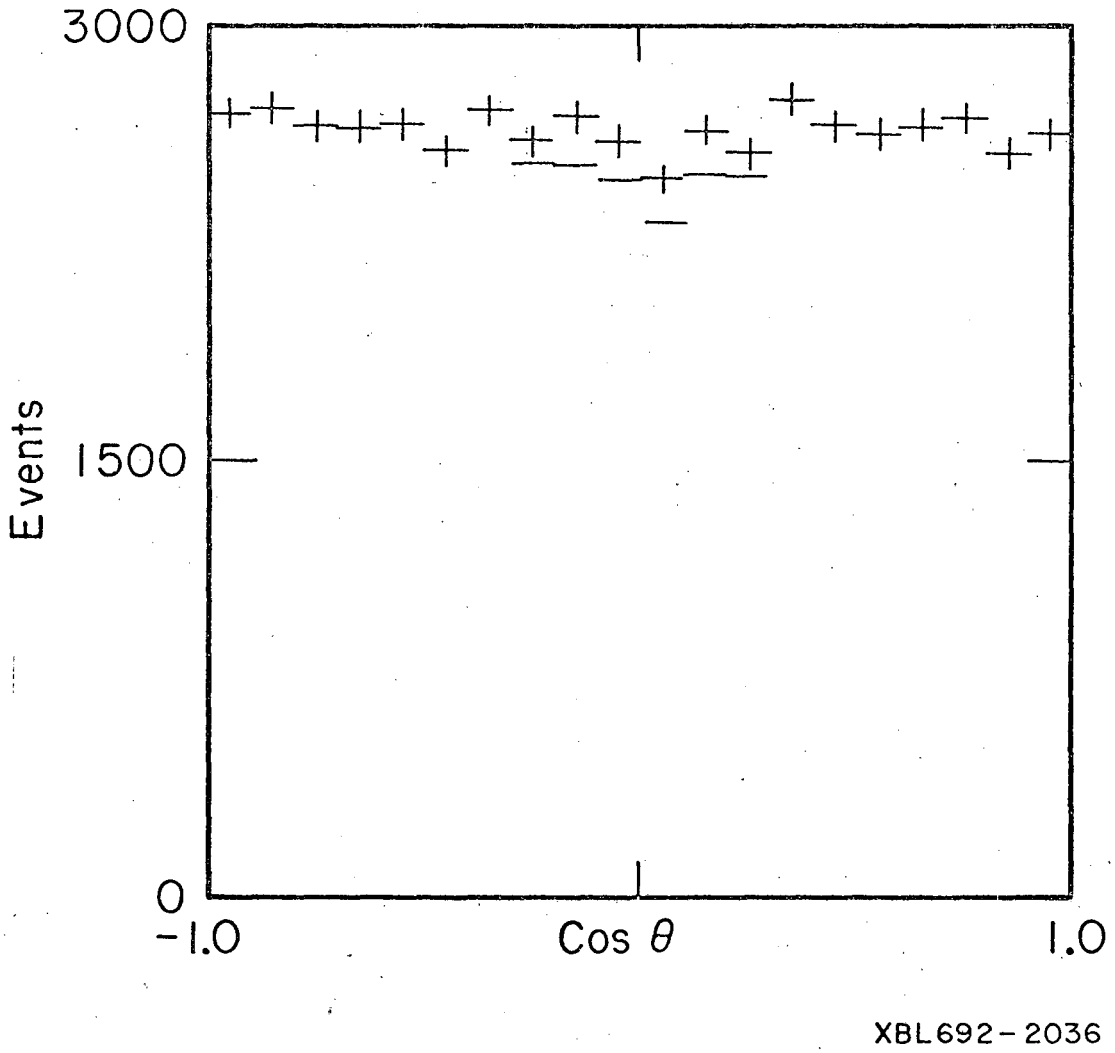

Fig. 3b

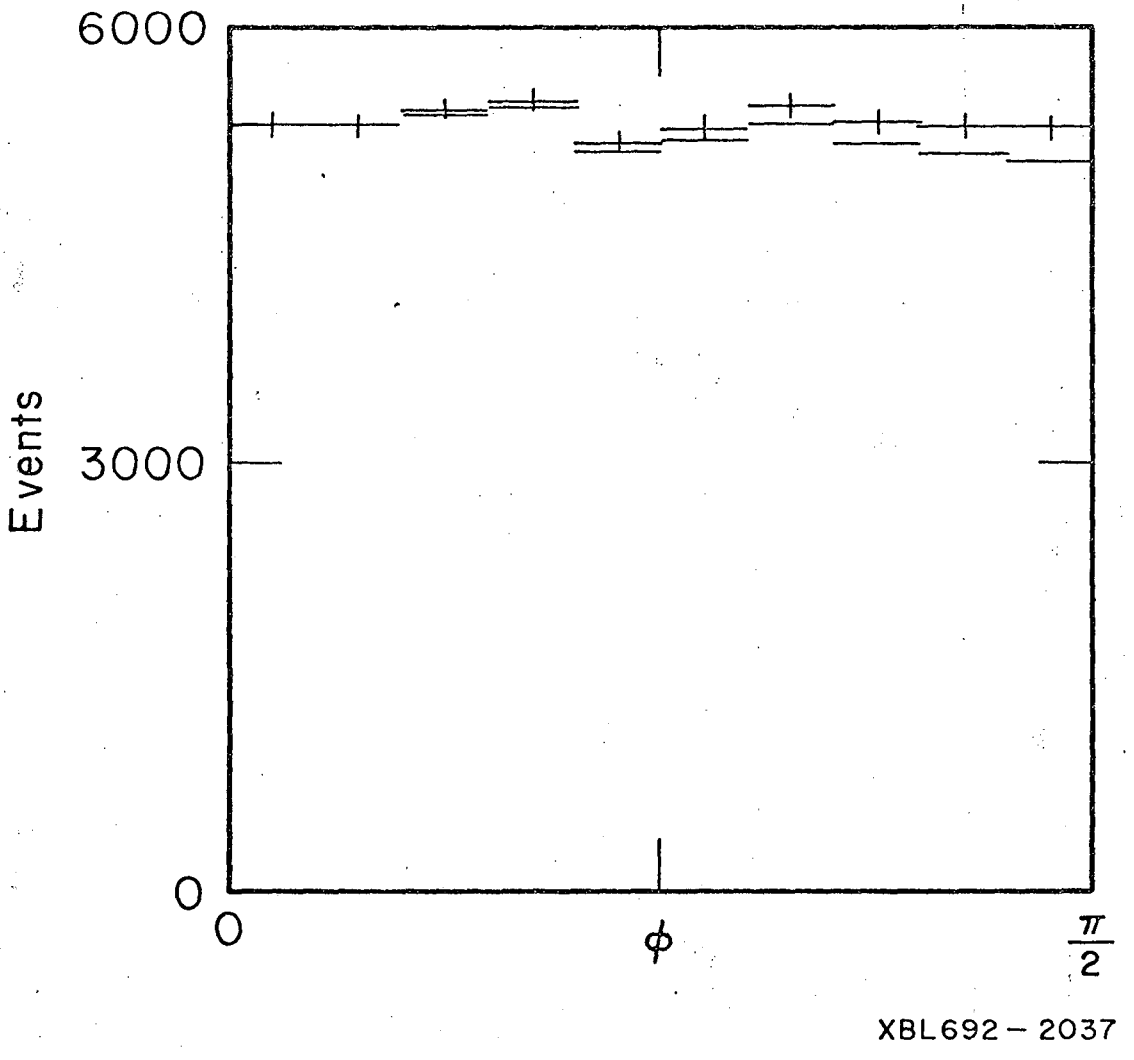

Fig. 3c

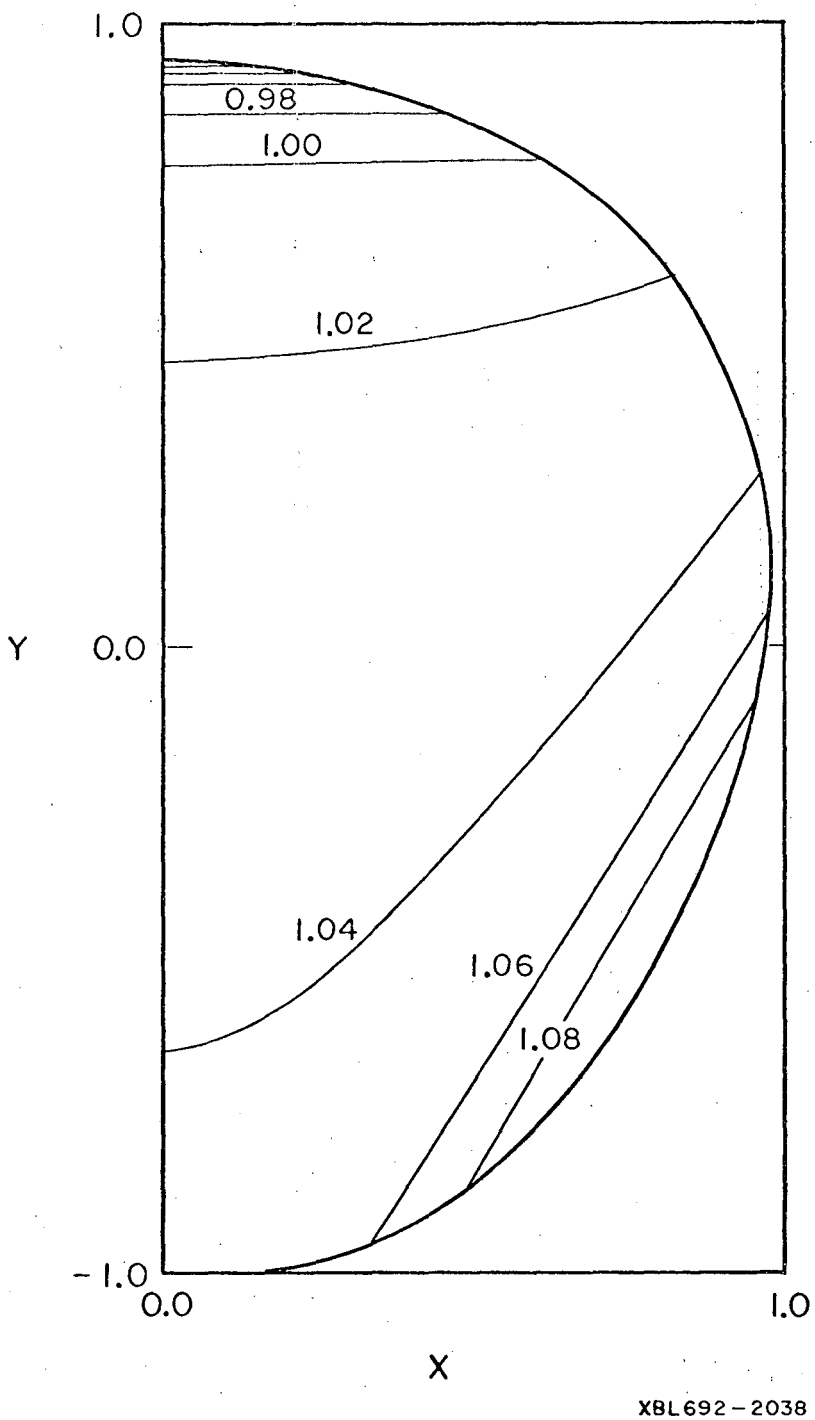

Fig. 4

0.924

170.7	192.0	195.1	172.0	157.0	134.9	98.3	87.1	60.6	18.5											
13.2	14.0	14.1	13.2	12.7	11.7	10.0	9.4	7.9	4.4											
180.4	191.6	197.9	183.7	212.7	193.7	208.4	204.5	197.6	202.1	188.9	120.9	66.2	18.6							
13.6	14.0	14.2	13.7	14.8	14.1	14.6	14.5	14.3	14.4	14.0	11.2	8.3	4.4							
173.6	203.3	198.4	213.3	197.1	201.5	189.6	182.5	196.1	192.2	186.2	189.4	172.9	194.8	121.3	34.2					
13.3	14.4	14.2	14.8	14.2	14.4	14.0	13.7	14.2	14.1	13.9	14.0	13.4	14.2	11.2	6.0					
206.0	188.8	186.7	207.1	197.7	179.4	193.1	169.4	209.1	181.3	193.8	175.3	181.5	202.2	199.3	189.8	106.8	13.5			
14.5	13.9	13.8	14.6	14.3	13.6	14.1	13.2	14.7	13.7	14.2	13.5	13.7	14.5	14.4	14.0	10.5	3.7			
185.4	183.3	209.4	188.7	200.4	195.3	174.1	186.4	192.0	185.7	194.0	190.0	155.7	178.6	204.6	176.5	177.5	155.7	35.3		
13.8	13.7	14.7	13.9	14.4	14.2	13.4	13.9	14.1	13.9	14.2	14.0	12.7	13.6	14.6	13.5	13.6	12.7	6.1		
177.8	173.8	197.7	181.1	194.8	177.2	190.9	191.1	202.4	188.1	187.1	206.6	169.3	171.4	198.5	201.4	190.9	206.5	171.0	13.5	
13.6	13.4	14.3	13.7	14.2	13.6	14.1	14.1	14.5	14.0	13.9	14.6	13.3	13.3	14.4	14.5	14.1	14.6	13.3	3.7	
150.4	188.2	182.8	161.0	177.8	182.7	162.1	156.9	193.1	190.1	168.3	209.8	154.8	196.3	174.4	169.1	166.1	180.5	188.6	99.5	
12.5	14.0	13.8	12.9	13.6	13.8	13.0	12.8	14.2	14.1	13.2	14.8	12.7	14.3	13.5	13.2	13.1	13.7	14.0	10.2	
191.4	170.2	173.1	179.0	188.2	161.2	162.2	166.1	188.4	158.1	179.6	172.5	162.9	167.1	193.0	151.4	208.4	198.0	163.6	147.0	
14.1	13.3	13.4	13.7	14.0	12.9	13.0	13.1	14.0	12.8	13.7	13.4	13.0	13.2	14.2	12.5	14.7	14.3	13.0	12.3	
148.3	169.7	153.3	163.7	168.7	172.1	178.9	169.2	166.4	186.7	162.0	182.6	173.2	186.6	179.2	175.0	169.9	174.8	173.7	165.3	
12.4	13.3	12.6	13.1	13.3	13.4	13.6	13.3	13.2	13.9	13.0	13.8	13.4	13.9	13.6	13.5	13.3	13.4	13.4	13.1	
170.7	189.5	175.8	146.1	161.7	170.7	171.5	164.0	132.9	170.9	178.0	158.5	162.4	173.8	164.4	165.1	162.1	177.5	183.5	150.4	
13.4	14.1	13.6	12.4	13.0	13.3	13.4	13.0	11.7	13.3	13.6	12.8	13.0	13.4	13.0	13.1	12.9	13.5	13.8	12.4	
183.2	189.2	151.7	169.3	161.2	168.5	174.6	151.6	152.2	164.2	163.5	158.1	162.0	157.7	160.5	170.8	182.0	158.3	164.4	93.5	
13.8	14.1	12.6	13.3	12.9	13.2	13.5	12.5	12.6	13.0	13.0	12.8	12.9	12.7	12.9	13.3	13.7	12.8	13.0	9.8	
164.1	153.0	189.8	175.8	178.0	128.8	165.9	169.1	147.7	148.7	167.8	180.0	166.1	157.0	155.8	157.8	137.1	150.3	151.4	22.5	
13.1	12.6	14.1	13.6	13.6	11.6	13.1	13.2	12.4	12.4	13.1	13.6	13.1	12.7	12.6	12.7	11.8	12.4	12.4	4.8	
159.0	157.5	187.6	185.2	156.6	151.7	179.1	137.3	172.1	137.8	158.1	171.1	141.3	143.1	131.2	164.2	188.4	150.6	76.3		
12.9	12.8	14.0	13.9	13.1	12.6	13.6	11.9	13.3	11.9	12.7	13.2	12.0	12.1	12.8	12.9	13.9	12.4	8.8		
144.9	145.6	171.3	167.0	157.6	152.0	148.7	146.5	165.7	155.3	160.0	148.2	128.7	163.9	172.0	167.7	160.6	88.4			
12.3	12.3	13.3	13.2	12.8	12.5	12.4	12.3	13.1	12.6	12.8	12.3	11.5	12.9	13.2	13.1	12.8	9.5			
144.7	160.9	158.7	126.6	146.4	140.8	175.8	142.5	157.5	151.7	156.8	156.6	137.6	163.9	158.7	156.3	82.2	1.0			
12.3	12.9	12.8	11.5	12.3	12.1	13.5	12.1	12.7	12.5	12.7	12.7	11.8	12.9	12.7	12.6	9.1	1.0			
163.1	167.3	126.8	136.0	152.5	134.6	161.2	136.3	151.4	147.0	136.5	161.6	143.9	145.7	150.4	47.7					
13.0	13.2	11.5	11.9	12.6	11.8	12.9	11.9	12.5	12.3	11.8	12.9	12.1	12.2	12.4	7.0					
137.2	147.6	141.3	152.5	161.9	127.3	161.5	151.9	151.6	124.4	136.5	156.6	130.9	86.7	16.3						
11.9	12.4	12.1	12.6	13.0	11.5	12.9	12.5	12.5	11.3	11.8	12.7	11.6	9.4	4.1						
146.4	127.8	145.4	127.6	144.2	151.2	133.5	127.1	138.3	158.7	127.5	92.3	15.3								
12.3	11.5	12.3	11.5	12.2	12.5	11.8	11.5	11.9	12.8	11.5	9.7	4.0								
136.1	146.3	127.7	121.4	136.9	128.4	132.5	143.7	90.9	43.3	11.3										
11.9	12.3	11.5	11.2	11.9	11.5	11.7	12.2	9.7	6.7	3.4										
126.5	122.4	105.9	113.0	92.2	54.9	32.1	1.0													
11.5	11.3	10.5	10.8	9.8	7.5	5.8	1.0													

Y

-1.0 0.0 X 0.965

Fig. 5a

XBL 692-237

UCRL-18760

0.924

184.0	205.1	205.8	179.4	163.0	139.6	101.2	89.2	61.8	18.9										
14.4	15.0	14.9	13.8	13.1	12.2	10.3	9.7	8.1	4.4										
181.3	192.4	198.7	184.1	213.5	194.5	209.1	205.2	198.2	202.7	189.2	120.7	66.0	18.5						
13.6	14.0	14.3	13.7	14.8	14.1	14.7	14.5	14.3	14.5	14.0	11.2	8.2	4.4						
172.2	201.6	196.8	211.5	195.5	199.8	188.0	180.9	194.4	190.3	184.4	187.5	171.1	192.7	119.8	33.7				
13.2	14.3	14.1	14.7	14.1	14.3	13.9	13.6	14.1	14.0	13.7	13.9	13.2	14.1	11.1	5.9				
203.0	186.0	184.0	204.1	194.8	176.8	190.3	166.9	205.9	178.4	190.8	172.4	178.5	198.7	195.7	186.3	104.7	13.2		
14.3	13.7	13.6	14.4	14.1	13.4	13.9	13.0	14.5	13.5	14.0	13.3	13.5	14.2	14.1	13.8	10.3	3.7		
182.0	179.9	205.5	185.2	196.7	191.7	170.8	182.8	188.3	182.0	190.1	186.1	152.4	174.8	200.1	172.4	173.3	151.8	34.3	
13.6	13.5	14.4	13.7	14.1	13.9	13.2	13.6	13.8	13.6	13.9	13.8	12.4	13.3	14.3	13.2	13.3	12.4	5.9	
174.0	170.1	193.4	177.2	190.6	173.4	186.8	186.9	197.9	183.8	182.7	201.7	165.2	167.1	193.4	196.1	185.7	200.6	165.9	13.1
13.3	13.1	14.0	13.4	13.9	13.3	13.8	13.8	14.2	13.7	13.6	14.3	12.9	13.0	14.0	14.1	13.7	14.2	12.9	3.6
146.9	183.8	178.5	157.2	173.6	178.3	158.2	153.0	188.3	185.3	164.0	204.3	150.6	190.9	169.5	164.1	161.0	174.7	182.2	96.0
12.2	13.7	13.5	12.6	13.3	13.4	12.7	12.5	13.8	13.7	12.9	14.4	12.3	13.9	13.1	12.9	12.7	13.2	13.5	9.8
186.6	165.9	168.7	174.4	183.4	157.0	157.9	161.7	183.4	153.8	174.6	167.6	158.2	162.0	187.0	146.5	201.3	190.9	157.4	140.9
13.8	13.0	13.1	13.3	13.6	12.6	12.6	12.8	13.6	12.5	13.3	13.0	12.6	12.8	13.7	12.1	14.2	13.8	12.5	11.8
144.3	165.1	149.2	159.2	164.0	167.3	173.9	164.4	161.6	181.2	157.1	177.0	167.7	180.5	173.1	168.8	163.5	167.8	166.2	157.3
12.1	13.0	12.3	12.7	12.9	13.0	13.3	12.9	12.8	13.5	12.6	13.3	13.0	13.5	13.2	13.0	12.8	12.9	12.8	12.4
165.8	184.1	170.8	141.9	157.0	165.7	166.4	159.0	128.8	165.5	172.3	153.3	156.9	167.7	158.4	158.7	155.4	169.5	174.2	141.9
13.0	13.7	13.2	12.0	12.6	12.9	13.0	12.7	11.4	12.9	13.1	12.4	12.5	12.9	12.6	12.5	12.4	12.9	13.1	11.7
177.7	183.5	147.1	164.2	156.2	163.3	169.1	146.8	147.2	158.8	157.9	152.6	156.1	151.7	154.1	163.5	173.5	150.1	154.6	87.0
13.4	13.6	12.2	12.9	12.6	12.8	13.0	12.2	12.1	12.6	12.6	12.3	12.5	12.3	12.3	12.7	13.0	12.1	12.2	9.1
159.0	148.1	183.8	170.2	172.2	124.6	160.5	163.4	142.6	143.4	161.7	173.2	159.6	150.5	149.0	150.2	129.7	140.9	139.4	20.5
12.7	12.2	13.6	13.1	13.2	11.2	12.7	12.8	11.9	12.0	12.7	13.1	12.5	12.2	12.1	12.1	11.2	11.6	11.5	4.4
153.8	152.3	181.4	179.1	151.0	146.5	172.9	132.4	165.8	132.7	152.0	164.3	135.3	136.6	153.2	155.1	176.0	137.1	67.9	
12.4	12.4	13.5	13.4	12.7	12.1	13.1	11.5	12.8	11.5	12.2	12.7	11.5	11.5	12.2	12.2	12.9	11.3	7.8	
139.9	140.6	165.4	161.2	152.1	146.6	143.3	141.0	159.3	149.1	153.3	141.7	122.7	155.5	162.2	156.1	145.7	74.1		
11.9	11.9	12.9	12.7	12.3	12.1	11.9	11.8	12.6	12.1	12.3	11.8	10.9	12.3	12.5	12.2	11.6	8.0		
139.5	155.1	153.0	121.9	141.0	135.5	169.0	136.9	151.1	145.3	149.7	149.1	130.4	154.1	147.4	139.6	65.5	.5		
11.8	12.5	12.4	11.0	11.9	11.6	13.0	11.7	12.2	11.9	12.1	12.1	11.2	12.1	11.8	11.3	7.3	.5		
157.0	161.1	122.0	130.8	146.6	129.3	154.6	130.5	144.8	140.2	129.7	152.9	135.1	134.8	134.4	39.3				
12.5	12.7	11.0	11.4	12.1	11.3	12.4	11.4	11.9	11.7	11.2	12.2	11.4	11.3	11.1	5.8				
131.8	141.8	135.7	146.4	155.2	122.0	154.5	145.1	144.4	118.1	128.9	146.6	120.6	78.2	14.1					
11.5	11.9	11.6	12.1	12.4	11.0	12.4	12.0	11.9	10.7	11.2	11.9	10.7	8.5	3.5					
140.4	122.5	139.3	122.2	138.0	144.5	127.3	120.8	131.0	149.6	119.2	85.4	13.9							
11.8	11.0	11.8	11.0	11.7	12.0	11.2	10.9	11.3	12.1	10.7	9.0	3.6							
130.2	140.0	122.1	115.9	130.6	122.3	125.7	135.9	85.6	40.5	10.5									
11.4	11.8	11.0	10.7	11.4	11.0	11.1	11.5	9.1	6.3	3.2									
120.8	116.8	100.9	107.6	87.7	52.1	30.4	1.0												
10.9	10.8	10.0	10.3	9.3	7.2	5.5	1.0												

Y

-1.0 0.0 X 0.965

Fig. 5b

XBL 692-236

UCRL-18760

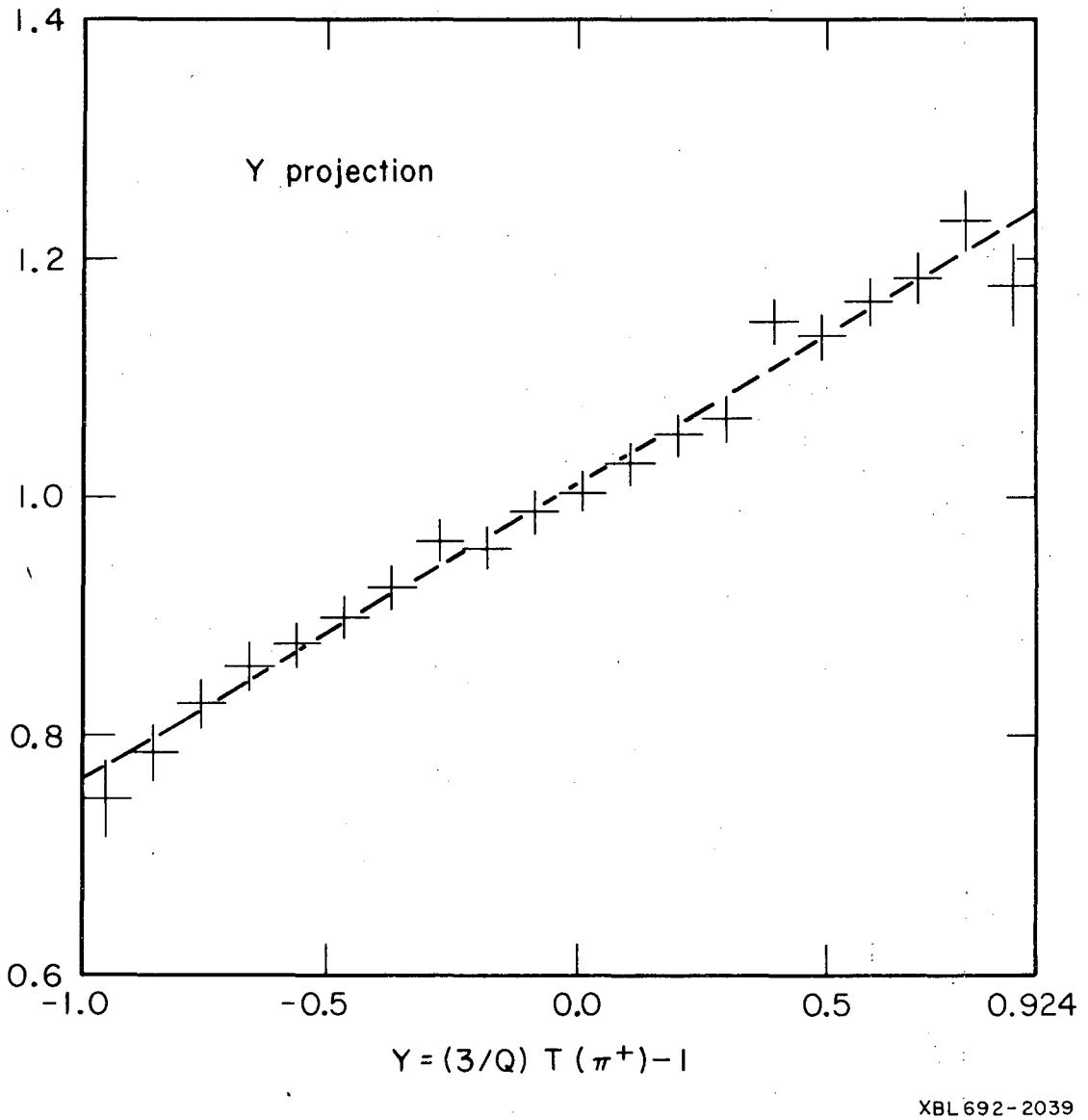

Fig. 6

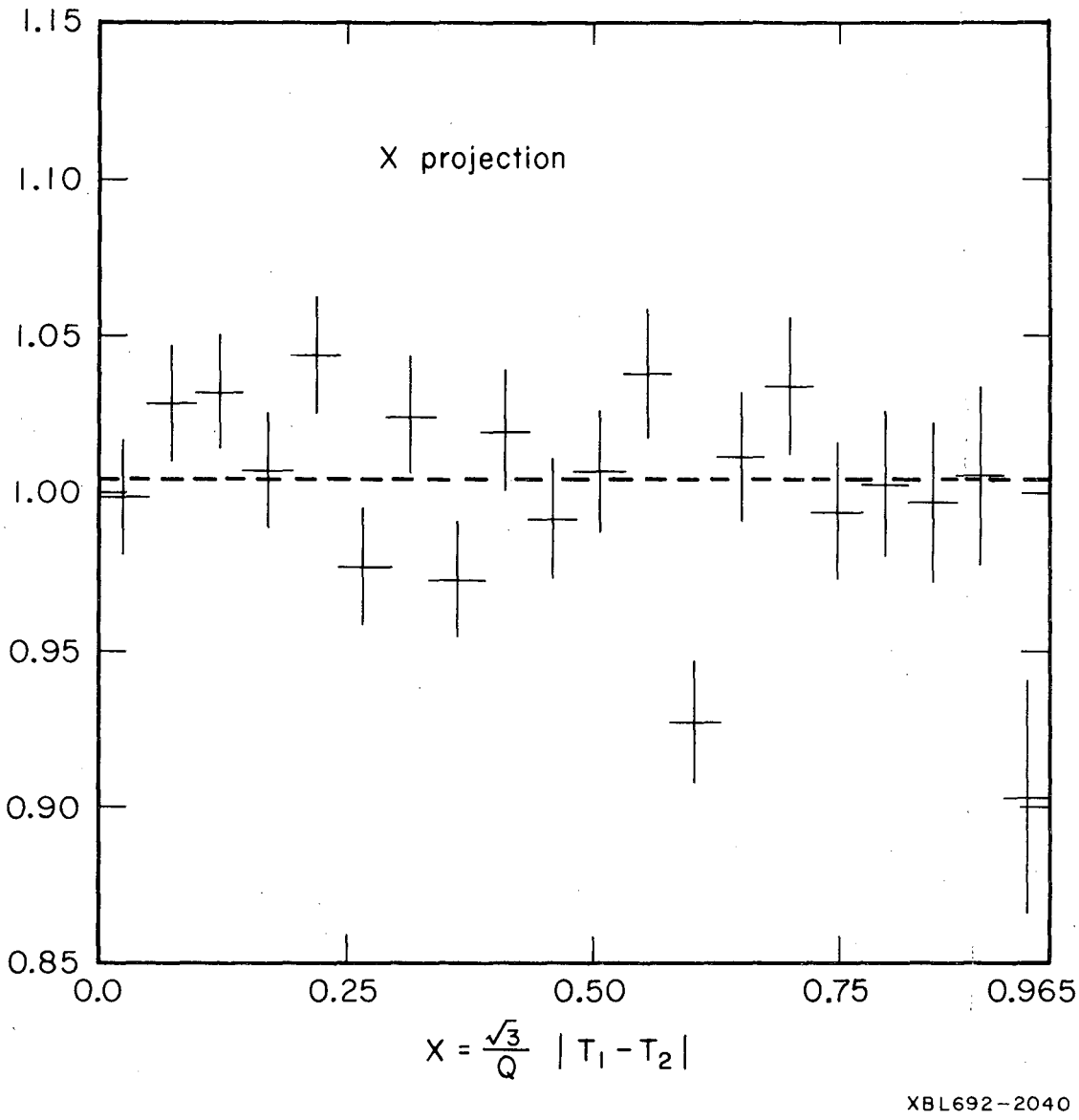
X projection
1.15
1.10
1.05
1.00
0.95
0.90
0.85
0.0
0.25
0.50
0.75
0.965
$X = \frac{\sqrt{3}}{Q} \mid T_1 - T_2 \mid$
XBL692-2040

Fig. 7

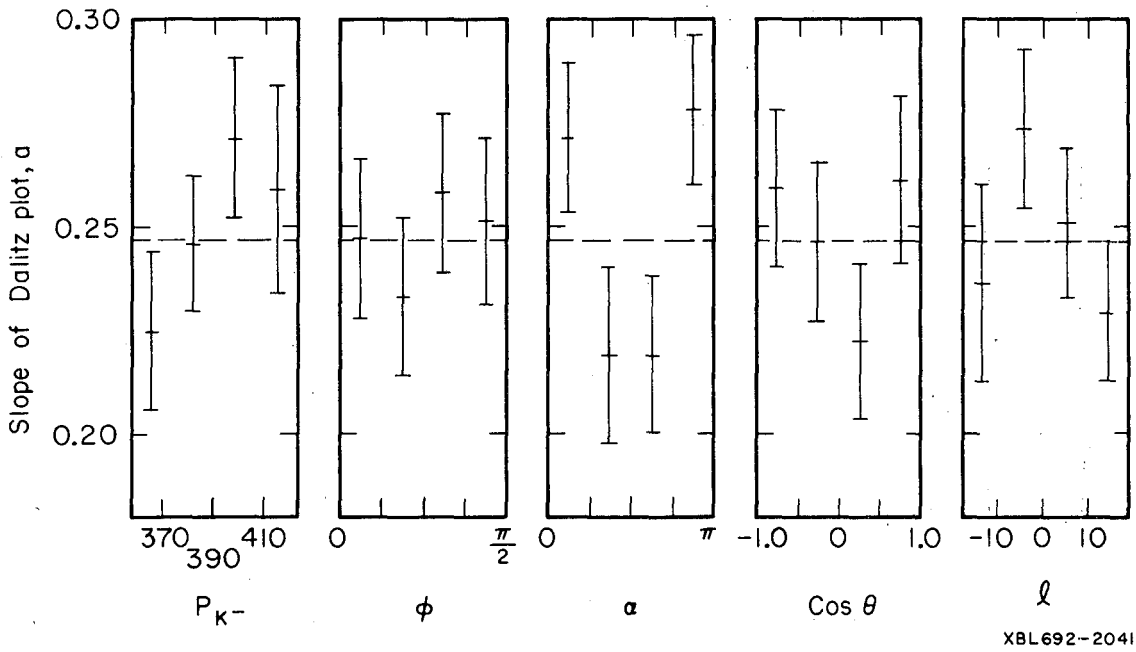
0.30
0.25
0.20
Slope of Dalitz plot, a
370
390
410
P_{K^-}
0
$\frac{\pi}{2}$
ϕ
0
π
α
-1.0
0
1.0
Cos θ
-10
0
10
ℓ
XBL692-2041

Fig. 8

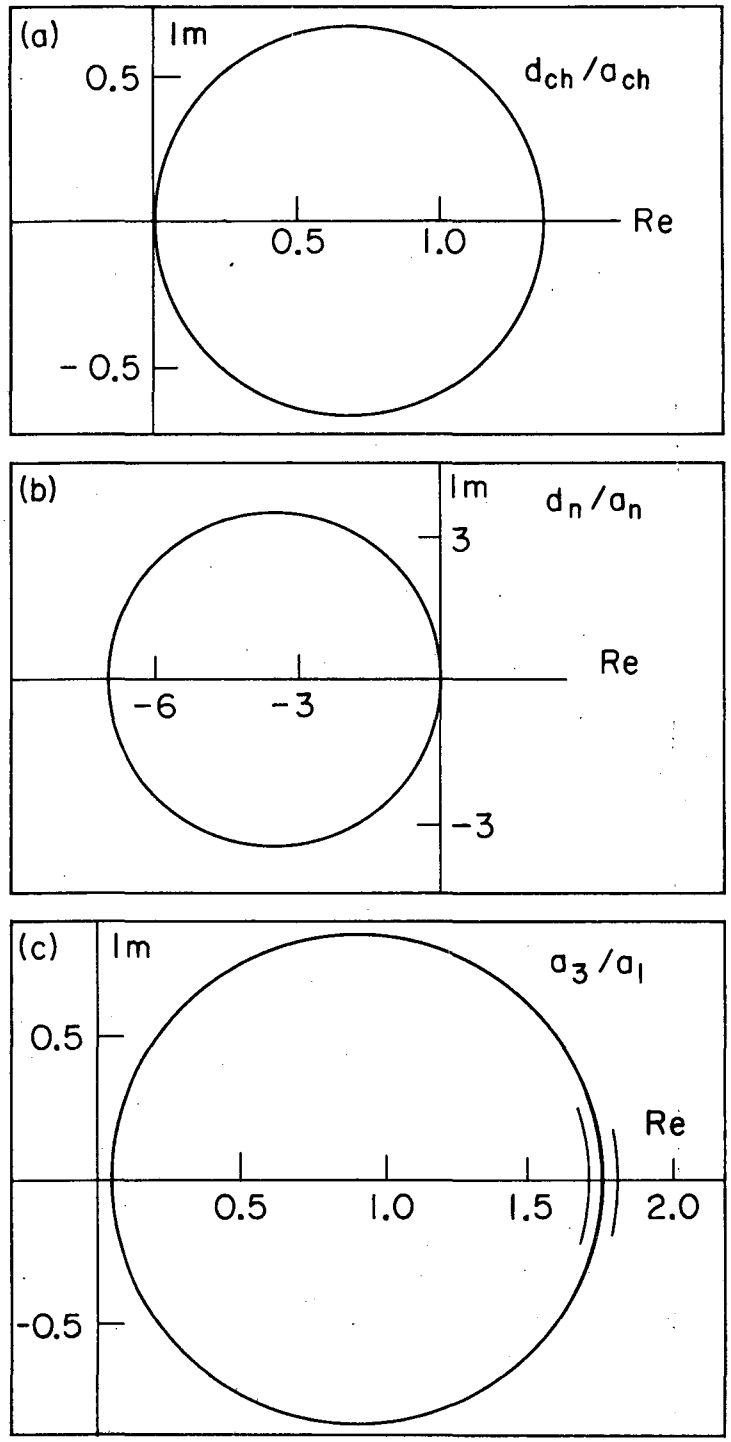
(a)
Im
0.5
d_{ch}/a_{ch}
Re
0.5
1.0
-0.5
(b)
Im
d_n/a_n
3
Re
-6
-3
-3
(c)
Im
a_3/a_1
0.5
Re
0.5
1.0
1.5
2.0
-0.5
XBL692-2042

Fig. 9

LEGAL NOTICE

This report was prepared as an account of Government sponsored work. Neither the United States, nor the Commission, nor any person acting on behalf of the Commission:

A. Makes any warranty or representation, expressed or implied, with respect to the accuracy, completeness, or usefulness of the information contained in this report, or that the use of any information, apparatus, method, or process disclosed in this report may not infringe privately owned rights; or

B. Assumes any liabilities with respect to the use of, or for damages resulting from the use of any information, apparatus, method, or process disclosed in this report.

As used in the above, "person acting on behalf of the Commission" includes any employee or contractor of the Commission, or employee of such contractor, to the extent that such employee or contractor of the Commission, or employee of such contractor prepares, disseminates, or provides access to, any information pursuant to his employment or contract with the Commission, or his employment with such contractor.

TECHNICAL INFORMATION DIVISION
LAWRENCE RADIATION LABORATORY
UNIVERSITY OF CALIFORNIA
BERKELEY, CALIFORNIA 94720